

# Interpenetrating Organometallic Polymer Networks Based on Poly(dimethylacrylamide-*co*-methylenebisacrylamide): Synthesis and ISEC-ESR Characterization

**M. Zecca**

*Dipartimento di Chimica Inorganica, Metallorganica e Analitica, via Marzolo 1, 35131 Padova, Italy*

**A. Biffis**

*Institut für Organische Chemie und Makromolekulare Chemie, Heinrich-Heine Universität Düsseldorf, Universitätstrasse 1, D-40225 Düsseldorf, Federal Republic Germany*

**G. Palma and C. Corvaja**

*Dipartimento di Chimica Fisica, via Loredan 2, 35131 Padova, Italy*

**S. Lora**

*Istituto F.R.A.E., C.N.R., 35020 Legnaro, Italy*

**K. Jeřábek\***

*Institute Chemical Processes Fundamentals Academy of Sciences of the Czech Republic, 165 02 Praha 6, Czech Republic*

**B. Corain**

*Dipartimento di Chimica, Ingegneria Chimica e Materiali, Università di L'Aquila, Italy, and Centro per lo Studio della Stabilità e Reattività dei Composti di Coordinazione, C.N.R., via Marzolo 1, 35131 Padova, Italy*

*Received December 12, 1995; Revised Manuscript Received April 1, 1996*<sup>⊗</sup>

**ABSTRACT:** Poly(*N,N*-dimethylacrylamide) resins, cross-linked up to 8 mol % with methylenebisacrylamide, have been investigated in the swollen state (dichloromethane, DCM, and tetrahydrofuran, THF) by means of inverse steric exclusion chromatography (ISEC) and electron spin resonance spectroscopy (ESR). Their behavior has been evaluated on the basis of a physicochemical model, which was previously developed to describe the behavior of the same materials in water. This model is based on the assumption that the swollen resins can be depicted as concentrated viscous polymer solutions. In DCM, this hypothesis still holds for the relatively lightly cross-linked swollen gels, while it is not acceptable when the cross-linking degree is higher than 4 mol %. When THF is used as the liquid medium, the investigated resins do not fully swell, and the spin probe employed for the ESR measurements is adsorbed from the liquid phase onto the polymer chains. Therefore, the characterization of these polymers swollen in THF did not give unambiguous results. The same ISEC–ESR combined approach has been exploited to study the swelling behavior of several sequential interpenetrating organometallic polymer networks. These materials were obtained upon dispersion of different amounts of an organometallic, cross-linked copolymer—*co*(vinylferrocene/*N,N*-dimethylacrylamide/methylenebisacrylamide)—inside a poly(*N,N*-dimethylacrylamide) resin, cross-linked with methylenebisacrylamide (4 mol %). The introduction of the “guest” copolymer into the tridimensional network of the resin has been found to increase the swelling volume of the “host” matrix.

## Introduction

We recently reported<sup>1,2</sup> on the synthesis of macromolecular composites resulting from the dispersion of a copolymer of vinylferrocene (VF) inside the macro- and microporous domains<sup>2</sup> of a poly(dimethylacrylamide) (DMA) resin cross-linked with 4 mol % methylenebisacrylamide (MBA). Analytical evaluations (elemental and X-ray microprobe analyses) coupled with electron spin resonance spectroscopy (ESR) and inverse steric exclusion chromatography (ISEC) examinations revealed that these composites are authentic sequential interpenetrating polymer networks materials<sup>3</sup> which, in spite of a fairly high polymer chain concentration, are accessible in the swollen state to molecules of substantial size.<sup>2,4</sup> Moreover, Mössbauer spectroscopy revealed

the perfect survival of the ferrocenyl chromophore, and chemical tests gave convincing evidence about the survival of its chemical reactivity as well.<sup>2,4</sup> These materials can be considered as model interpenetrating organometallic polymer networks (IOPNs)<sup>2</sup>, novel metalloorganic copolymers potentially useful in metal-catalyzed organic synthesis.<sup>5</sup> However, for a rational design of IOPN-based catalysts, an accurate knowledge of their macromolecular structure in the swollen state is needed. In fact, this has a decisive influence on the transport phenomena within the catalyst, and therefore on its overall catalytic activity.

We have also reported on a combined ESR–ISEC analysis of a number of poly(DMA-*co*-MBA) resins containing different proportions of the cross-linking comonomer.<sup>6</sup> We proposed a physicochemical model which rationalizes the observed phenomenological correlation between ESR and ISEC outcomes, and we

<sup>⊗</sup> Abstract published in *Advance ACS Abstracts*, May 15, 1996.

**Table 1.**  
**Poly(dimethylacrylamide)-*co*-methylenabisacrylamide)**  
**Matrices: Analytical Data**

matrix	composition	nominal degree of cross-linking, mol %	irradiation time, h
M1	5.914 g of DMA 0.093 g of MBA	1	142
M2	5.819 g of DMA 0.185 g of MBA	2	142
M3	5.772 g of DMA 0.276 g of MBA	3	142
M4	11.52 g of DMA 0.688 g of MBA	4	142
M6	5.457 g of DMA 0.542 g of MBA	6	72
M8	5.283 g of DMA 0.713 g of MBA	8	72

proved that these water-swollen polymer networks can be rationally and quantitatively described as concentrated aqueous "solutions" of polymer chains. This model of the swollen polymer structure has been found to be applicable to other microporous resins as well.<sup>7</sup>

We report in this paper on the experiments aimed at further testing our model and at getting some insight on how the macromolecular structure and the chemical accessibility of a resin are modified when a "guest" organometallic copolymer is introduced in the tridimensional network to yield an IOPN material. This information could be valuable for better understanding the macromolecular structure of sequential IOPNs.

## Experimental Section

**Materials.** DMA and VF were obtained from Aldrich. MBA was supplied by Janssen. Solvents were purchased from Carlo Erba. All the chemicals were used as received, apart from THF, which was distilled over Na prior to use.

**Apparatus.** Grinding of the materials was performed with a Bühler HO4 impact grinder. Scanning electron microscopy (SEM) and X-ray microanalysis (XRM) were carried out on a Cambridge Stereoscan 250 EDX PW 9800 apparatus. ESR spectra were recorded on a Bruker ER 200D X-band spectrometer. Elemental analyses (C, H, N) were carried out by means of a Carlo Erba 1106 analyzer. Atomic absorption measurements (Fe) were performed with a Perkin Elmer 3030 atomic adsorption spectrophotometer. ISEC measurements were carried out using a standard chromatographic setup described elsewhere.<sup>8</sup>

**Synthesis of the Resins M1–M8.** The resins were synthesized at 195 K by exposure of the comonomer mixtures to the  $\gamma$ -rays from a <sup>60</sup>Co source. The composition of the monomer mixtures and the irradiation times are reported below (Table 1). The resins were obtained as cylindrical rods, which underwent extensive self-breaking in methanol. After self-breaking had apparently stopped, the resins were repeatedly washed with methanol, acetone, and diethyl ether and dried to constant weight. Polymerization yields were quantitative in all cases. The materials were then suspended in water and ground by impact grinding to a particle size smaller than 0.2 mm; the finest particles were eliminated by repeated decantation in water.

**Synthesis of the IOPN Composites C1–C3.** Resin M4 was employed as the "host" copolymer, without previous grinding. The required amount of resin was swollen with a solution of DMA, MBA, and VF in *N,N*-dimethylformamide (DMF). The molar ratios of the three comonomers were kept constant for all the composites (14.1 mol % VF, 81.6 mol % DMA, 4.3 mol % MBA). The volume of the solution was chosen in such a way as to minimize the presence of any free solution after impregnation. The residual solution was separated by simply pouring it from the polymerization flasks, which were subsequently exposed to  $\gamma$ -rays from a <sup>60</sup>Co source at room temperature for 72 h. The resulting materials were repeatedly washed with methanol and acetone and dried to constant

**Table 2. IOPN Materials: Analytical Data**

IOPN	polymerization mixture	yield, <sup>a</sup> %	guest copolymer content, wt %	iron content, wt %
C1	3.204 g of M4 0.963 g of mm <sup>b</sup> 4.274 g of DMF	53	14	0.9
C2	2.596 g of M4 1.559 g of mm 3.320 g of DMF	68	29	1.5
C3	2.200 g of M4 1.995 g of mm 2.361 g of DMF	62	36	2.4

<sup>a</sup> Computed from comparison of the weight of the monomer mixture and the actually determined difference between the resulting IOPN and the starting matrix. <sup>b</sup> mm, monomer mixture (14.1 mol % VF, 81.6 mol % DMA, 4.3 mol % MBA).

weight. Polymerization yields and other data relevant to the syntheses are reported in Table 2. Grinding of the IOPN materials with the impact grinder was unsatisfactory (the desired particle size smaller than 0.2 mm was not achieved). Therefore, these materials were ground with a mortar and pestle after swelling in DCM. As for the matrices, the finest particles were then eliminated by decantation.

**Atomic Absorption Measurements.** Metal contents were determined by atomic absorption spectrometry on solutions obtained by digestion of a weighted amount of composite in hydrogen peroxide (120 vol)/sulfuric acid 5/1 (v/v), followed by dilution to a concentration suitable for the measurements.

**ISEC Measurements.** Full details on sample preparations and on chromatographic runs are given elsewhere.<sup>8,9</sup> Deuterium oxide, sugars, and polydextrans were employed as standard solutes when water was used as the mobile phase, whereas linear C3–C30 hydrocarbons and linear polystyrenes were used in dichloromethane and tetrahydrofuran.

**ESR Measurements.** The sample of ground resins were swollen with a nitrogen-saturated 10<sup>−4</sup> M solution of TEMPONE in the selected solvent. The samples were allowed to reach swelling equilibrium, and then, the excess solution was removed by filtration under a nitrogen atmosphere, and the swollen samples were placed in the ESR tube. Each spectrum was obtained as the sum of 10 scans. The temperature was varied in steps 10–20 K in the range 310–270 K for water-swollen, 295–195 K for DCM-swollen, and 295–175 K for THF-swollen polymers, waiting at least 10 min between subsequent measurements to ensure a proper thermostating of the sample. Spectra were taken both while decreasing and while increasing the temperature, in order to check for the reproducibility of the spectra. Rotational correlation times  $\tau$  were calculated according to the following formula:<sup>10</sup>

$$\tau = 175 \times 10^{-9} \times [1 - \sqrt{h(+1)/h(-1)}]DH(+1) \quad (1)$$

The parameters  $h(+1)$ ,  $h(-1)$  (amplitudes of the low- and high-field spectral lines, respectively) and  $DH(+1)$  (width of the low-field spectral line) were obtained directly from the derivative spectrum by peak-picking. The numerical constant was estimated on the basis of published values for the anisotropic  $g$  and  $A$  tensors for TEMPONE.<sup>11</sup>

## Results

**Synthesis of the Matrices and of the IOPN Composites.** Batch polymerization of mixtures of DMA and MBA at 195 K under  $\gamma$ -ray irradiation easily yielded the cross-linked matrices M1–M8; the data relevant to the syntheses are reported in Table 1.

SEM analysis (up to 5000 magnification) revealed for all the matrixes the expected compact vitreous morphology. Less cross-linked materials were elastic and appeared rather opaque, while the more cross-linked resins were more rigid and transparent.

Resin M4 was chosen as the "host" matrix for the preparation of four different IOPN materials (Table 2).

They were obtained by dispersing different amounts of the organometallic "guest" copolymer through the host polymer network. In this case, the observed polymerization yields were far from quantitative (50–70%). This can be attributed in part to the incomplete incorporation of the monomer mixture in the matrix prior to polymerization (see Experimental Section) and possibly also to the relatively short irradiation time employed. The figures for the iron content analysis were essentially proportional to the VF content in the polymerization mixture. XRM analysis on IOPN C2 showed quite homogeneous metal distribution throughout the IOPN particles.

To confirm that no additional cross-linking due to radical formation on the host polymer chains was formed during the synthesis of IOPNs, a sample of matrix M4 was swollen in DMF and then irradiated at room temperature for 72 h. The postirradiated resin was then swollen with a water solution of TEMPONE and characterized by ESR spectroscopy (see below). The observed correlation time was not higher than it was in the case of the nonirradiated matrix. We have already demonstrated that the value of  $\tau$  observed for TEMPONE in water-swollen poly(DMA) resins depends on the distribution of polymer chain density throughout the swollen polymer mass.<sup>6</sup> As the distribution pattern apparently depends on the cross-linking degree of the resins, this result clearly indicates that the postirradiation has not practically affected the structure and the morphology of matrix M4. Moreover, the polymerization yield in the formation of the guest has never been quantitative. This means that molecules of comonomers (DMA, VF) are always present during the irradiation. It must be appreciated that the self-cross-linking of the host implies the coupling of two radical sites produced by  $\gamma$ -rays on the polymeric chains. This is a termination step, which should be much slower than the radical propagation step involving the monomer molecules (as long as they are present). Thus, it can be expected that, during the copolymerization which yields the guest, a potential further cross-linking of the host would be quenched. On the other hand, this consideration points out the possibility of grafting of the guest chains to the host ones. However, our earlier study<sup>2</sup> has shown that when VF and DMA were, in the absence of any cross-linker, copolymerized inside a 4% cross-linked poly(DMA) resin, the guest could be completely removed from the obtained material simply by washing it with a proper solvent. This finding rules out the occurrence of grafting, because it shows that this kind of guest can be permanently entrapped in this kind of host only when it forms a cross-linked network.

**ISEC Characterization of Matrices M1–M8 in DCM and THF.** As in our previous investigations,<sup>3,6</sup> the macromolecular structure of the samples of all materials herein reported will be described on the basis of a model composed of five discrete polymer fractions, each characterized by its volume  $V$  and polymer chain concentration  $C$  (0.1, 0.2, 0.5, 1.0, and 2.0 nm<sup>3</sup>/nm<sup>3</sup>). The obtained ISEC patterns for the swollen matrices in water, DCM, and THF are shown in Figure 1. All the matrices appear to be bidisperse materials, in which the total swollen gel volume is composed mainly of two domains. The more swollen one is characterized by  $C = 0.5$  nm<sup>-2</sup>, while the other, microporous domain has  $C = 2.0$  nm<sup>-2</sup>. As expected, the more cross-linked the resin, the larger the relative volume of the domain with the higher chain concentration.

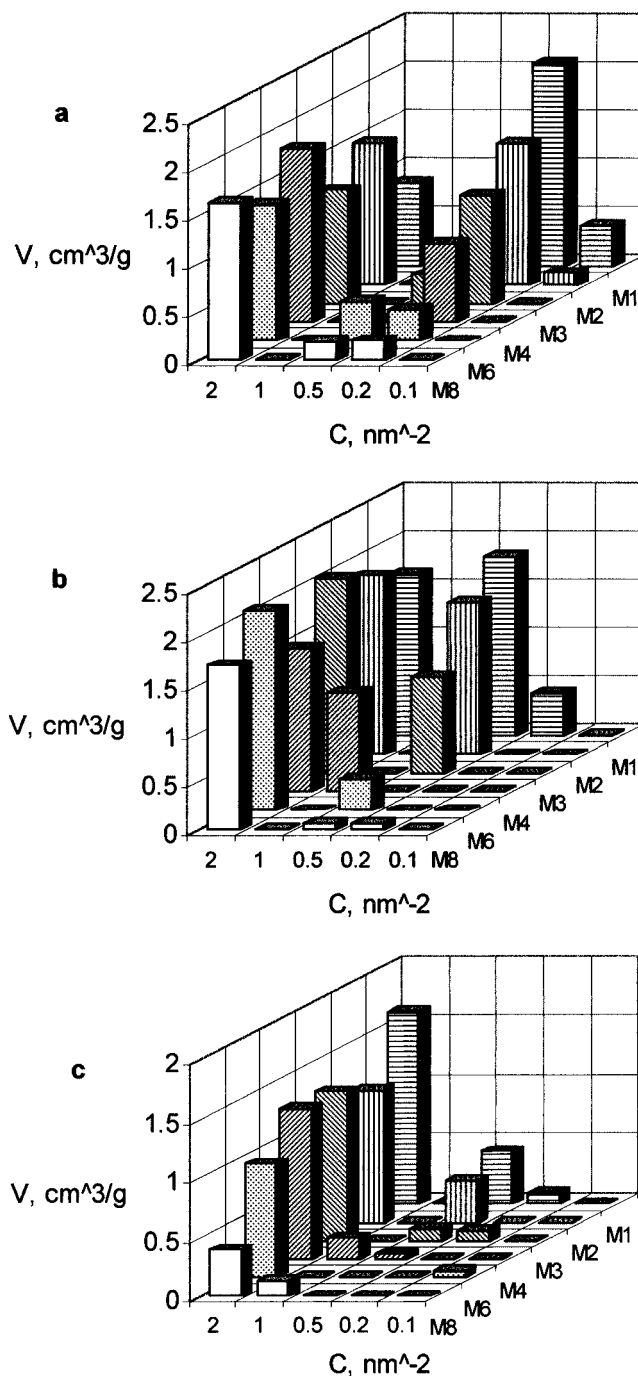


**Figure 1.** Volume distributions of variously dense polymer fractions in the matrices, as determined by ISEC in (a) water, (b) DCM, and (c) THF.

In an ideal case, the sum of the volumes of individual fractions, as calculated from the ISEC data, should be equal to the actual volume of the swollen polymer. The latter can be directly extracted from the chromatographic data as the difference of the volume of the empty chromatographic column and the elution volume of the biggest standard solute, totally excluded from the polymer. In Table 3, these data are compared for all the matrices in the three solvents.

The sum of the volumes of the individual fractions, as derived from the ISEC modeling of the polymer morphology (columns B, Table 3), never exceeds the actual volume of the swollen polymers. In particular, an acceptably good agreement between the values of both quantities was found in water and DCM. This supports the reliability of the employed model of mor-

**Table 3. Comparison of the Directly Measured Total Swollen Polymer Volumes (A) and the Sums of Volumes of the ISEC-Detected Polymer Fractions (B) for Matrices M1–M8**

matrix	volume in water, cm <sup>3</sup> /g		volume in DCM, cm <sup>3</sup> /g		volume in THF, cm <sup>3</sup> /g	
	A	B	A	B	A	B
M1	3.76	3.39	4.14	3.98	2.25	2.16
M2	3.21	3.06	3.40	3.43	1.79	1.47
M3	2.88	2.60	3.07	3.02	1.73	1.46
M4	2.60	2.63	2.64	2.50	1.60	1.50
M6	2.28	2.13	2.39	2.39	1.57	1.01
M8	2.02	1.99	2.16	1.82	1.29	0.52

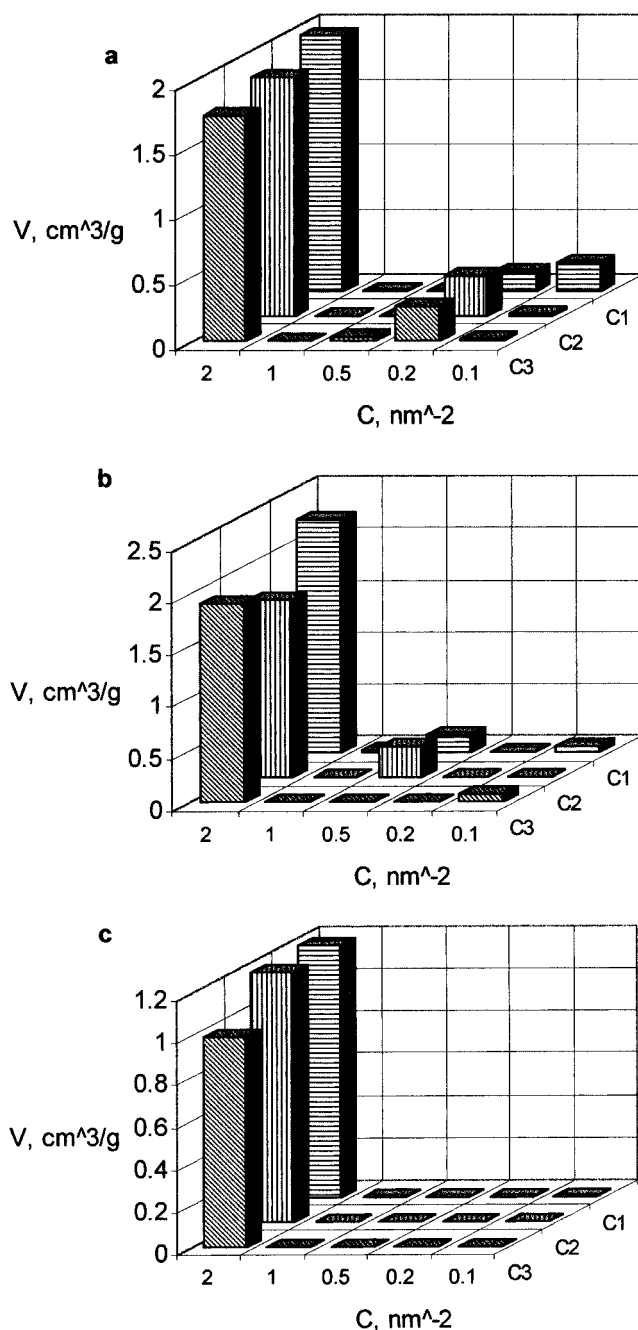
phology. In THF, an acceptable agreement of the computed and actual swollen gel volumes was found only for the least cross-linked matrix, M1. The higher the cross-linking degree of the matrix, the greater the difference between the actual and the computed swollen polymer volume. This is due to the fact that the ISEC-derived model can describe only the polymer domains participating to the chromatographic process. THF is apparently a bad swelling solvent for the investigated polymers, and the proportion of unswollen polymer mass, from which solutes are excluded, is likely to increase as the cross-linking degree increases. Therefore, under such conditions, ISEC fails to detect sensible fractions of the polymer mass in the more cross-linked materials.

**ISEC Characterization of IOPN Materials in Water, DCM, and THF.** The ISEC pattern of the composites in the three solvents is depicted in Figure 2. As expected, the relative volumes of the domains with lower chain concentration are dramatically reduced in the IOPN materials with respect to the pure host matrix. In fact, the interchain space, which was originally void in the present resin, has been occupied by the guest organometallic copolymer.

The values of the volume of the total swollen polymer mass as directly measured and as computed from ISEC output (see above) are shown in Table 4 for the precursor (matrix M4) and the three composites. The satisfactory agreement between the values of the two quantities in water and DCM, which was observed for M4, was found in the same swelling solvents also in the case of the composites. Accordingly, the incorporation of the guest copolymer in the host network does not prevent a reliable ISEC characterization of the IOPNs, at least not in water and DCM. The situation is different in THF, and the results of ISEC characterization of the composites are analogous to those achieved for the relatively highly cross-linked matrices swollen in the same solvent.

Swelling volume values are usually referred to the unit mass of dry polymeric material. However, since we are interested in studying the effect of the introduction of the guest copolymer in the matrix, the comparison of the values of experimental swelling volumes in much more meaningful if they are reduced to the unit mass of host matrix; these normalized values are reported in Table 5.

Apparently, the swelling volume of the host matrix increases as the weight proportion of the guest increases. This circumstance should occur if the swollen guest copolymer cannot be accommodated inside the swollen host network. Therefore, the swelling of the guest component generates additional tensions, which force the host matrix to swell to a higher extent in comparison with the pure resin.

**Figure 2.** Volume distribution of variously dense polymer fractions in the composites, as determined by ISEC in (a) water, (b) DCM, and (c) THF.**Table 4. Comparison of the Directly Measured Total Swollen Polymer Volumes (A) and Sums of Volumes of the ISEC-Detected Polymer Fractions (B) for Composites C1–C3 and Their Precursor, Matrix M4<sup>a</sup>**

polymer	volume in water, cm <sup>3</sup> /g		volume in DCM, cm <sup>3</sup> /g		volume in THF, cm <sup>3</sup> /g	
	A	B	A	B	A	B
M4	2.60	2.63	2.64	2.50	1.60	1.50
C1	2.19	2.33	2.40	2.45	1.61	1.18
C2	2.13	2.17	2.12	2.07	1.53	1.17
C3	1.99	2.05	2.00	1.99	1.56	0.99

<sup>a</sup> A, directly measured total swollen polymer volume. <sup>b</sup> B, swollen polymer volume computed from the ISEC results.

As a general comment, it must be emphasized that the introduction of a host cross-linked copolymer in a guest matrix of similar chemical nature to form a sequential IOPN does not cause any additional cross-

**Table 5. Directly Measured Total Swollen Volumes Related to 1 g of the Host Matrix**

polymer	water, cm <sup>3</sup> /g	DCM, cm <sup>3</sup> /g	THF, cm <sup>3</sup> /g
M4	2.60	2.64	1.60
C1	2.54	2.79	1.87
C2	3.00	2.98	2.15
C3	3.10	3.12	2.44

**Table 6. Rotational Correlation Time and Activation Energies of TEMPONE inside Matrices M1–M8 Swollen in DCM**

sample	$\tau$ at 295 K (ps)	$E_a$ (kJ mol <sup>-1</sup> )
bulk solution	25	
M2	50	13
M2	60	15
M3	67	15
M4	133	13
M6	203	14
M8	272	13

linking effect. However, its consequences are complex and can lead to an increase in the swelling volume of the host component, as it is in the case of our materials. It would be interesting to investigate the situation in which host and guest copolymers are of a substantially different chemical nature; studies about *simultaneous* IOPNs with these characteristics have already been published.<sup>13</sup>

**ESR Characterization of Matrices M1–M8 in DCM and THF.** As pointed out above, a previous combined ISEC–ESR investigation on matrices M1–M8 swollen in water showed that ISEC data can be quantitatively correlated with the rotational mobility of the paramagnetic probe TEMPONE (2,2,6,6-tetramethyl-4-oxopyridine-1-oxyl) dissolved in water and dispersed throughout the microporous domains of the investigated resins.<sup>6</sup> This was accomplished through the development of a physicochemical model of our microporous materials which fitted the experimental data remarkably well. Moreover, the model led to a predicted molecular radius for TEMPONE equal to 0.32 nm, in excellent agreement with the value 0.32 nm determined by other authors on the basis of a quite independent procedure.<sup>13</sup> This successful fitting lends promising support for our model, which depicts swollen light- and medium-cross-linked polymer networks as concentrated viscous “solutions” of polymer chains.

We tried then to extend these considerations to the characterization of the matrices in solvents other than water, namely, DCM and THF. The ESR spectra in DCM appeared to be uncomplicated and quite similar to those observed in water.<sup>3,6</sup> The rotational mobility of TEMPONE on going from M1 to M8 undergoes a clear reduction (see Table 6). The apparent activation energies are practically constant from M1 to M8. This is an indication that the hindrances to the motion of TEMPONE are of the same nature in all the matrices. These data were correlated with the ISEC information utilizing the previously developed model:<sup>6</sup>

$$\tau/\tau_0 = \sum [K_i V_i A^{C_i} / \sum K_i V_i] \quad (2)$$

where  $\tau/\tau_0$  is the ratio of the rotational correlation times inside of the gel and in free solution, respectively,  $V_i$  is the volume of  $i$ th fraction of the polymer mass, whose polymer chain concentration is  $C_i$ , and  $K_i$  is the Ogston's equilibrium distribution coefficient between the liquid phase and the  $i$ th fraction of polymer mass<sup>13</sup> for a certain chemical species, which is a function of its molecular size and of  $C_i$ . It was found that at a low

**Table 7. Values of the Parameter  $A$  for Matrices M1–M8 Swollen in DCM**

M1	M2	M3	M4	M6	M8
2.24	2.26	2.19	3.01	3.40	3.71

cross-linking degree (up to M3), the fitting of the model to the data was very satisfactory. However, the model was unable to correlate the data for the more cross-linked matrices M4, M6, and M8. This can be clearly seen by calculating the adjustable parameter  $A$  in our model for each matrix separately. In principle, it should have the same value for all the matrices. Using the value 0.32 nm for the radius of TEMPONE,<sup>8,14</sup> the values of  $A$  reported in Table 7 were obtained. It is apparent that the parameter remains practically constant on going from M1 to M3 and then begins to rise significantly. We speculate that the highly cross-linked matrices swollen in DCM cannot be depicted as concentrated polymer solutions, which is the fundamental assumption of our model. This means that above 3% cross-linking, the structure of our matrices gradually changes from a concentrated solution-like situation to one more typical of a porous solid with fixed structure<sup>15</sup> (“compartmentalization” of the matrix<sup>16</sup>). We are now trying to rationalize these findings by appropriate modifications of our model.

In contrast to the results obtained in DCM and water, in THF the ESR spectra are no longer uncomplicated, presenting at room temperature an anomalous line broadening. At low temperature, the spectra are resolved into two superimposed sets of signals, one of which is due to TEMPONE in fast rotation, as in water and DCM, while the other one is typical of an immobilized spin probe (Figure 3). This circumstance prevents an unambiguous determination of  $t$  and therefore of the rotational mobility. We speculate that this spectral pattern reveals the occurrence of an equilibrium between molecules of TEMPONE dissolved in confined THF, which are relatively free to rotate, with molecules chemisorbed on the polymer chains. A similar chemisorption of the spin probe on the polymer chain giving rise to complex spectra has already been reported.<sup>17</sup> These findings have discouraged ESR investigations on the IOPN materials in THF.

**ESR Characterization of the IOPN Materials.** The spectra of the IOPN composites swollen in water turned out to be complex. They are the sum of two sets of signals, attributable to radicals with similar mobility but slightly differing in their hyperfine splitting constants and  $g$  values. This complexity is particularly evident in the high-field line of the spectra, which appears remarkably distorted (Figure 4). Since the value of the splitting constant is dependent on the polarity of the environment surrounding the probe,<sup>18</sup> the spectra observed in the case of the IOPNs reveal that TEMPONE is distributed between two chemically different microenvironments, one of which is probably due to the host component, the other one to the guest component.

Complex spectra arising from heterogeneous macromolecular structures have been already reported in the literature.<sup>19</sup> However, they were usually interpreted in terms of heterogeneity in the cross-linking density, in that they indicated the simultaneous presence of radicals with much different mobility. In any case, much work remains to be done before quantitative conclusions can be drawn from such spectra.

The ESR spectra of TEMPONE dispersed inside C1–C3 are uncomplicated when DCM is the swelling

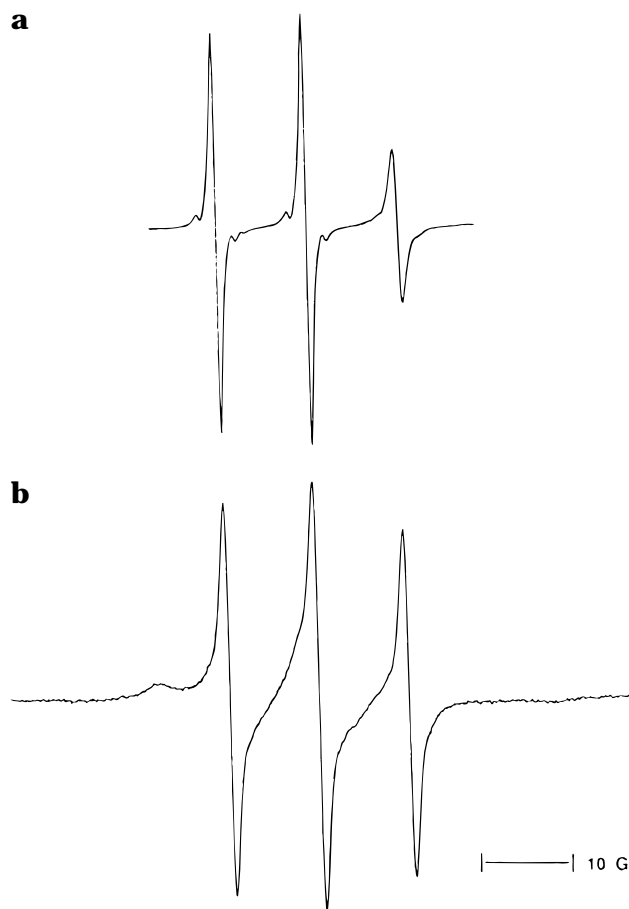


**Figure 3.** ESR spectra of TEMPONE in matrix M8 swollen in (a) DCM and (b) THF.

solvent. In fact, they are quite similar in shape to those observed inside matrices M1–M8. The reason for this uncomplicated behavior with respect to water can be twofold. Either in DCM the spin probe molecules rapidly exchange between the microenvironments with different polarity, so that averaged signals are detected at relatively high temperature, or the polarity differences in DCM are so small as to be negligible. The fact that the spectra remain also uncomplicated at low temperatures supports the latter explanation. The values of the apparent activation energies and the  $t$  values at 295 K are collected in Table 8. As in the case of the matrices, the apparent activation energies are practically the same for all the materials. The experimental values of  $t$  are generally close to one another, although the value observed for C3 is slightly higher than those obtained for the others, as was expected on the basis of the ISEC results, since the average chain concentration was quite the same for all the materials.

### Conclusions

We have further tested the potentialities of our combined ESR–ISEC approach in the characterization of the macromolecular structure of swollen microporous resins. Our conclusions can be summarized as follows:

Our model depicting the water-swollen polymer network as a concentrated polymer solution was found to apply also for lightly cross-linked matrices swollen in DCM. With increasing cross-linking, a more complicated model is needed, in order to account for the increasing rigidity of the network. Unfortunately, it was not possible to extend this analysis to THF, where TEMPONE appears to be adsorbed on the polymer

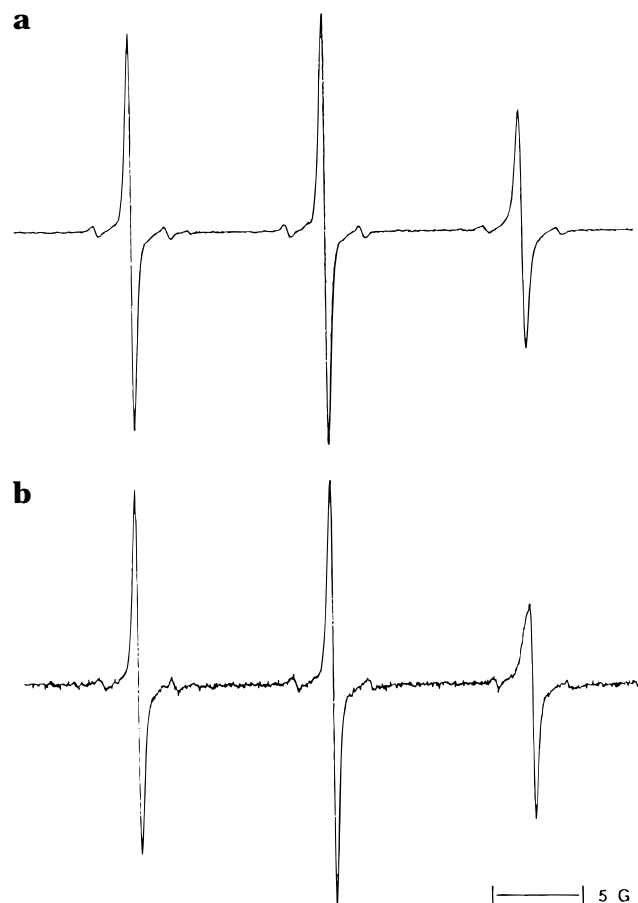


**Figure 4.** ESR spectra of TEMPONE in (a) water-swollen matrix M4 and (b) composite C3.  $T = 295$  K.

**Table 8. Rotational Correlation Time and Activation Energies of TEMPONE inside Matrices C1, C2, and C3 Swollen in DCM**

sample	$\tau$ at 295 K (ps)	$E_a$ (kJ/mol <sup>-1</sup> )
M4	133	13
C1	136	14
C2	145	14
C3	185	15

chains. However, a proper choice of the spin probe should overcome this problem.

Under proper conditions, the ESR technique turned out to be a sensitive tool for the detection of chemical heterogeneity in the resin, although the extrapolation of quantitative information from the obtained spectra appears to be rather laborious at the moment.

The study of the modifications of the macromolecular structure caused by the introduction of a “guest” cross-linked copolymer yielded some interesting results. The presence of the guest can increase the swelling volume of the “host” copolymer, yielding a material with a possibly better chemical accessibility than a normal resin with comparable chain concentration. This advantage adds to other positive features of the IOPN materials<sup>2,4,5</sup> and contributes to increase the interest for the IOPNs as potential novel heterogeneous catalysts.

**Acknowledgment.** This work was partially supported by Progetto Finalizzato Chimica Fine II and by MURST-40% funding and by Grant No. 104/94/0749 from the Grant Agency of the Czech Republic.

### References and Notes

- (1) Arshady, R.; Corain, B.; Lora, S.; Palma, G.; Russo, U.; Sam, F. O.; Zecca, M. *Adv. Mater.* **1990**, *2*, 412.

- (2) Corain, B.; Jerabek, K.; Lora, S.; Palma, G.; Zecca, M. *Adv. Mater.* **1992**, *4*, 97.
- (3) Sperling, L. H. *CHEMTECH* **1988**, 104.
- (4) Corain, B.; Corvaja, C.; Lora, S.; Palma, G.; Zecca, M. *Adv. Mater.* **1993**, *5*, 367.
- (5) Corain, B.; Zecca, M.; Biffis, A.; Lora, S.; Palma, G. *J. Organomet. Chem.* **1994**, *475*, 283.
- (6) Biffis, A.; Corain, B.; Zecca, M.; Corvaja, C.; Jerabek, K. *J. Am. Chem. Soc.* **1995**, *117*, 1603.
- (7) Biffis, A.; Corain, B.; Cvengrosova, Z.; Hronec, M.; Jerabek, K.; Kralik, M. *Appl. Catal. A* **1995**, *124*, 355.
- (8) Jerabek, K. *Anal. Chem.* **1985**, *57*, 1595; 1598.
- (9) Jerabek, K.; Setinek, K. *J. Polym. Sci. A* **1990**, *28*, 1387.
- (10) Bailey, P.; Gillies, D. G.; Sutcliffe, L. H. *J. Chem. Soc., Faraday Trans.* **1990**, *86*, 3309.
- (11) Brustolon, M.; Maniero, A. L.; Corvaja, C. *Mol. Phys.* **1984**, *51*, 1269.
- (12) Rogovina, L.; Zhou, P.; Frisch, H. L. *J. Polym. Sci. A* **1993**, *31*, 515.
- (13) Ogston, A. G. *Trans. Faraday Soc.* **1958**, *54*, 1754.
- (14) Hwang, J. S.; Mason, R. P.; Hwang, L. P.; Freed, J. H. *J. Phys. Chem.* **1975**, *79*, 489.
- (15) Meares, P. In *Diffusion in Polymers*; Crank, J., Park, G. S., Eds.; Academic Press: New York, 1968.
- (16) Watanabe, T.; Yahagi, T.; Fujiwara, S. *J. Am. Chem. Soc.* **1980**, *102*, 5187. Windle, J. J.; Scherrer, R. *Magn. Reson. Chem.* **1992**, *30*, 927.
- (17) Golikov, V. P.; Popkov, Yu. M.; Murontsev, V. I.; Nikolaev, N. I. *Zhur. Fiz. Khim.* **1972**, *46*, 2436. Lifshits, M. I.; Komarov, E. V. *Zhur. Fiz. Khim.* **1984**, *58*, 2593.
- (18) See, for example: Berliner, L. J., Ed. *Spin Labeling, Theory and Application*; Academic Press: New York, 1976.
- (19) Brown, I. M.; Sandreczki, T. C. *Macromolecules* **1985**, *18*, 2702. Pilar, J.; Horak, D.; Labsky, J.; Svec, F. *Polymer* **1988**, *29*, 500. Chachaty, C.; Soulie, E.; Wolf, C. *J. Chim. Phys.* **1991**, *88*, 153.

MA951825+